Available online at www.sciencedirect.com
ScienceDirect
Composites: Part A 38 (2007) 1473–1482
composites
Part A: applied science and manufacturing
www.elsevier.com/locate/compositesa

The effect of types of maleic anhydride-grafted polypropylene (MAPP) on the interfacial adhesion properties of bio-flour-filled polypropylene composites

Hee-Soo Kim, Byoung-Ho Lee, Seung-Woo Choi, Sumin Kim, Hyun-Joong Kim *

Laboratory of Adhesion and Bio-Composites, Program in Environmental Materials Science, Seoul National University, Seoul 151-921, South Korea

Received 12 August 2006; received in revised form 8 January 2007; accepted 9 January 2007

Abstract

The effect of processing temperature on the interfacial adhesion, mechanical properties and thermal stability of bio-flour-filled, polypropylene (PP) composites was examined as a function of five different maleic anhydride-grafted PP (MAPP) types. To investigate the effect on the interfacial adhesion of the composites, the five MAPP types were subjected to characterization tests. The MAPP-treated composites with sufficient molecular weight and maleic anhydride (MA) graft (%) showed improved mechanical and thermal stability. The enhanced interfacial adhesion, and mechanical and thermal stability of the MAPP-treated composites was strongly dependent on the amount of MA graft (%) and the MAPP molecular weight. The morphological properties of the MAPP-treated composites showed strong bonding and a paucity of pulled-out traces from the matrix in the two phases. In addition, the improved interfacial adhesion of the MAPP-treated composites was confirmed by spectral analysis of the chemical structure using attenuated total reflectance (FTIR-ATR). The crystallinity of PP, MAPP, MAPP-treated composites and non-treated composites was investigated using wide-angle X-ray scattering (WAXS) and differential scanning calorimetry (DSC).

Keywords: A. Thermoplastic resin; E. Extrusion; B. Mechanical properties; E. Thermal analysis

1. Introduction

In recent years, bio-filler-filled thermoplastic polymer composites have been widely studied for the application and development of environmentally friendly materials in line with the rising environmental consciousness worldwide [1–3]. The composites have several advantages such as environmental superiority, low cost, low density, lower manufacturing energy, low CO_2 emission, renewability and biodegradability, compared to inorganic-filler reinforced thermoplastic polymer composites [2–5]. Rice husk flour (RHF) and wood flour (WF) are considered two bio-fillers. Especially, RHF is an agricultural waste material generated in rice-producing countries in the Asian, Pacific and North American regions. The composites have predominant dimensional stability under moisture exposure, termite resistance and high resistance to biological attack compared to wood-based materials. Due to these superior properties, composites are being used increasingly in the building industry for sidings, window and door frames, decks, interior paneling, and automotive interior parts such as door panels, trunk liners, and door trims [1,6,7].

The main disadvantage of using composites is the low compatibility between the hydrophilic character of the polar bio-filler and hydrophobic character of the non-polar matrix polymer [2]. Bio-fillers do not disperse easily in thermoplastic polymers such as polyolefin and biodegradable polymer. Due to strong intermolecular hydrogen bonding between bio-fillers, they tend to agglomerate during the

* Corresponding author. Tel.: +82 2 880 4784; fax: +82 2 873 2318.
E-mail address: hjokim@snu.ac.kr (H.-J. Kim).

1359-835X/$ - see front matter © 2007 Elsevier Ltd. All rights reserved.
doi:10.1016/j.compositesa.2007.01.004

compounding process with the matrix polymer. The low compatibility and interfacial adhesion of composites lead to low mechanical and thermal properties of the final products [9–11]. Therefore, the study of ways to improve the interfacial adhesion between bio-fillers and matrix polymers is very important for the application of composites in industrial materials. In recent years, the various methods that have been studied to improve the interfacial adhesion of composites, by modifying the bio-filler surface, have included the use of maleic anhydride-grafted polypropylene (MAPP) [2], the addition of silane coupling agents [12], grafting matrix polymer with hydrophilic functional group [9], chemical modification of bio-filler surface [8,10,11] and plasma treatment of the bio-filler surface [13]. The use of MAPP, which is a very effective compatibilizer for bio-filler and matrix at the interface, has been the most common method to improve interfacial adhesion. The maleic anhydride (MA)-grafted, thermoplastic polymer increases the polarity which leads to better adhesion with bio-fillers [2]. The mechanical and thermal properties of MAPP-treated composites are likely to be different from those of MAPP in terms of molecular weight, MA graft (%), and melt flow index (MFI). Thus, five types of commercially used MAPP were investigated in this study.

The objective of this research was to investigate and compare the interfacial adhesion of different MAPP-treated composites. We used five types of MAPP that are commercially used in industries requiring enhanced adhesion. In particular, we evaluated MAPP characterization to investigate its effect on the interfacial adhesion of composites. We compared the mechanical properties, thermal properties, and effect of manufacturing temperature of MAPP-treated and non-treated composites as a function of different MAPP types. The crystallinity of PP, MAPP, MAPP-treated and non-treated bio-composites was determined by WAXS and differential scanning calorimetry (DSC). We determined that selecting the proper MAPP type is an important step in improving the interfacial interaction of composites.

2. Experimental

2.1. Materials

Polypropylene (PP) was supplied by Hyosung Co., South Korea. It has an MFI of 1.7 g/10 min (190 °C/2160 g) and a density of 0.91 g/cm^3. The bio-fillers used as the reinforcing filler were RHF and WF, obtained from Saron Filler Co. and Dong Yang CMI Co., South Korea, respectively. The particle size of RHF was 860–270 μm and that of WF was 110 μm. Table 1 shows the chemical constituents of bio-flour. The five types of MAPP were obtained from Eastman Chemical Products, Co. (Epolene G-3003 and E-43), Crompton Polybond, Co. (Polybond 3150 and Polybond 3200), and Polyram, Co. (Bondyram 1004), respectively.

Table 1
Chemical constituents of bio-flour

	Others (%)	Holocellulose (%)	Lignin (%)	Ash (%)
Wood flour[a]	10.9	62.5	26.2	0.4
Rice husk flour[b]	6.3	59.9	20.6	13.2

[a] Wood flours from Ref. [2].
[b] From Saron Filler Co.

2.2. Compounding and sample preparation

RHF and WF were oven dried at 105 °C for 24 h to adjust the moisture content to 1–3% and then stored in sealed polyethylene bags before compounding. PP was blended with the RHF and WF in a laboratory-sized, co-rotating, twin-screw extruder using three general processes: melt blending, extrusion and pelletizing. The extruder barrel was divided into eight zones with the temperature in each zone being individually adjustable. The temperature of the mixing zone in the barrel was maintained at 190 °C with a screw speed of 250 rpm. The extruded strand was cooled in a water bath and pelletized using a pelletizer. Extruded pellets were oven dried at 80 °C for 24 h and stored in sealed polyethylene bags to avoid unexpected moisture infiltration. The RHF and WF application level was 30 wt%, based on the total weight, prior to compounding. The five types of MAPP, used as the compatibilizing agent, were applied at 3 wt% based on the total weight of bio-flour and PP. Extruded pellets were injection molded into tensile (ASTM D638), Izod impact (ASTM D256), and three-point bend test bars (ASTM D790) using an injection molding machine (Bau Technology, South Korea) at 190 °C with an injection pressure of 1200 psi and a device pressure of 1500 psi. The tensile specimen had the following dimensions: $W = 3.18 \pm 0.03$ mm, $L = 9.53 \pm 0.03$ mm, $G = 7.62 \pm 0.02$ mm, $T = 3.00 \pm 0.08$ mm, where W is the width of the narrow section, L the length of the narrow section, G the gage length, and T the thickness of the narrow section. After injection molding, the test bars were conditioned before testing at $50 \pm 5\%$ RH for at least 40 h according to ASTM D 618-99.

2.3. MAPP characterization

2.3.1. Molecular weight of MAPP

Three of the MAPP types, Polybond 3150, Polybond 3200 and Bondyram 1004, were eluted using 1,2,4-trichlorobenzene (TCB) as the eluent solvent at 170 °C at a flow rate of 1 mL/min. Molecular weights were measured by GPC at 170 °C using a PL-GPC 210 system (Polymer Laboratories) equipped with refractive index (RI) detectors and a PL-gel 10 μm column (two mixed-B). The weight-average molecular weights (M_w) were calculated using a calibration curve from polystyrene standards. M_w of G-3003 and E-43 were obtained from Eastman Chemical Products Co.

2.3.2. Melt flow index (MFI) of MAPP

MFI values of the five MAPP types were measured at 190 °C with a load of 2.16 kg following ASTM D1238 using a melt indexer (Tinius Olsen Co., USA).

2.3.3. Melting temperature (t_m) and glass transition temperature (t_g) of MAPP

DSC analysis was carried out using a TA Instrument DSC Q 1000 (NICEM at Seoul National University) with 5–8 mg of each different MAPP type. Each sample was scanned from −80 to 200 °C at a heating rate of 10 °C/min and then cooled at the same rate under a nitrogen atmosphere. Two thermal properties, T_m and T_g, were determined from the second scan. T_m was defined to be the maximum of the endothermic melting peak from the heating second scan and T_g as the deflection of the baseline in the cooling second scan.

2.3.4. Thermogravimetric analysis (TGA) of MAPP

TGA measurements were carried out using a thermogravimetric analyzer (TA instruments, TGA Q500) on 5-mg samples of the different MAPP types, over a temperature range from 25 to 700 °C, at a heating rate of 20 °C/min. TGA was conducted with the compounds placed in a high quality nitrogen (99.5% nitrogen, 0.5% oxygen content) atmosphere at a flow rate of 40 ml/min in order to avoid unwanted oxidation.

2.4. Mechanical property tests of composites

The tensile test for the composites was conducted according to ASTM D 638-99 with a Universal Testing Machine (Zwick Co.) at a crosshead speed of 100 mm/min and a temperature of 24 ± 2 °C. Notched Izod impact strength was measured on an impact tester (Dae Yeong Co.) by ASTM method D 256-97 at room temperature. The three-point bend tests of the composites were carried out in accordance with ASTM D 790. The specimen had a span to depth ratio of 16:1. The composites were tested at a crosshead speed of 5 mm/min. Five measurements were conducted and averaged for the final result.

2.5. Morphological test

Scanning electron microscopy (SEM) was used to measure the fracture surfaces of the MAPP-treated and non-treated tensile specimens using a SIRIOM scanning electron microscope (FEI Co., USA). Prior to the measurement, the specimens were coated with gold (purity, 99.99%) to eliminate electron charging.

2.6. Thermogravimetric analysis (TGA) of composites

The thermal degradation and stability of the MAPP-treated and non-treated composites according to manufacturing temperature and time were measured by the isothermal condition of TGA. TGA measurements were carried out using the same TGA Q500 analyzer on 8–10 mg samples, over a temperature range from 25 °C to 180, 200 and 220 °C, at a heating rate of 20 °C/min, under a nitrogen flow of 40 ml/min. After ramping to the targeting temperature (180, 200 and 220 °C), the composites underwent isothermal testing for 20 min. TGA was measured with the composites placed in a high quality nitrogen (99.5% nitrogen, 0.5% oxygen content) atmosphere to prevent unwanted oxidation.

2.7. Attenuated total reflectance (FTIR-ATR) measurements

The infrared spectra in the FTIR-ATR of G-3003, Bondyram1004, the composites and G-3003-treated composites were obtained using a Thermo Nicolet Nexus 870 FTIR spectrophotometer (USA). A diamond was used as the ATR crystal. The samples were analyzed over the range of 525–4000 cm^{-1} with a spectrum resolution of 4 cm^{-1}. All spectra were averaged over 32 scans. This analysis of the composites was performed at point-to-point contact with a pressure device.

2.8. Differential scanning calorimetry (DSC) analysis of composites

DSC analysis was carried out using a TA Instrument DSC Q 1000 (NICEM at Seoul National University) with 5–8 mg of each composite. Each sample was scanned from −80 to 200 °C at a heating rate of 10 °C/min and then cooled at the same rate under a nitrogen atmosphere.

The specimens' relative percentage of crystallinity (X_c) was calculated according to the following equation:

$$X_c = \frac{\Delta H_f 100}{\Delta H_f^0 w}$$

where ΔH_f is the heat of fusion of the PP, MAPP and composites, ΔH_f^0 is the heat of fusion for 100% crystalline PP ($\Delta H_{100} = 138$ J/g) [14] and w is the mass fraction for PP in the composites.

2.9. X-ray analysis

Wide-angle X-ray scattering (WAXS) analysis of PP, MAPP, MAPP (G-3003)-treated and non-treated composites was performed with a Bruker General Area Detector Diffraction System (GADDS; NICEM at Seoul National University) that recorded the intensity of the X-rays diffracted by the sample as a function of the Bragg angle using Bruker computer software. Cu Kα radiation with wavelength $\lambda = 1.54$ Å was used with a nickel filter. The exposure time was 300 s with a 0.02 (°2θ) step. Two-dimensional scattering patterns were obtained by means of a Hi-Star X-ray detector. The crystallinity index (or percentage of apparent crystallinity; C.I.%) of the composites was calculated as follows [15]:

$$CI\% = (A.cryst./A.total) \times 100$$

A.cryst. is the corresponding area of the peak due to crystal diffraction of the sample and A.total is the total area; crystal and amorphous of the sample diffractograms.

3. Results and discussion

3.1. Characterization of MAPP types

MA-maleated PP has been widely used as a compatibilizing agent and adhesion promoter for bio-filler filled polypropylene composites. The MA functional group which grafts on the PP backbone acts as the chemical link between the hydrophobic matrix polymer and the hydrophilic surface of bio-flour. Table 2 shows M_w, MA graft (%), MFI, T_g and T_m of the five commercially used, MAPP types investigated in this research. The characterization of MAPP differed according to the kind of MAPP processing method. Due to this variation of basic MAPP properties, we expected that the mechanical properties and interfacial adhesion of the composites would be affected by MAPP type.

The M_w of Bondyram 1004 and G-3003 and the MA graft (%) of G-3003 and E-43 were the highest, while the M_w of E-43 and MA graft (%) of Polybond 3150 were the lowest. According to MAPP types, the difference of M_w could be seen that M_w varied according to MAPP type and processing method. The mechanical properties of MAPP-treated composites were affected by the M_w and MA graft (%) of MAPP. Low M_w MAPP does not sufficiently diffuse and entangle with the PP matrix. Excessively high M_w MAPP may not allow the coupling agent to reside at the interface between MAPP and PP matrix. The low MA graft (%) of MAPP did not offer sufficient interaction and hydrogen bonding between the anhydride group of MAPP and bio-filler. Excessively high MA graft (%) of MAPP may hold the coupling agent too close to the hydrophilic surface and not allow sufficient interaction with the continuous matrix phase [6,15]. These results confirmed the non-optimum mechanical properties of MAPP-treated composites with excessively low or high M_w and MA graft (%). Therefore, the sufficient polymer backbone M_w and MA graft (%) of MAPP is more easily diffused into the matrix polymer and provides enough sites for attachment to the polar bio-flour, respectively. The final properties and interfacial adhesion of MAPP-treated composites with sufficient M_w and MA graft (%) were superior to those of MAPP with low or excessively high M_w and MA graft (%) [6,15–18]. The MFI of MAPP was affected by the M_w, polydispersity and MA graft (%) of MAPP. Although they showed similar M_w, Polybond 3200 had the highest MFI while Polybond 3150 had the lowest, possibly because Polybond 3200 has lower M_w and polydispersity and higher MA graft (%) content. The polydispersity of Polybond 3150 and Polybond 3200 was 5.8 and 4.3, respectively. However, we did not measure the MFI of E-43 due to its very low M_w and high MFI. The high MFI value of MAPP slightly increased the production rate of composites in the melt mixing process using twin-screw extruder. T_m of E-43 was the lowest due to its low M_w. T_g did not show any significant variation among the five MAPP types.

Fig. 1 shows TGA curves of the five MAPP types. The thermal stability and decomposition temperature of Polybond 3200 were higher than those of Bondyram 1004, Polybond 3150 and G-3003, even though its M_w was lower than that of Bondyram 1004, Polybond 3150 and G-3003, possibly because the thermal stability of the base PP of Polybond 3200 was the highest. In addition, the thermal stability of E-43 was the lowest due to its extremely low M_w. Nowadays, the commercial use of MAPP to improve the interfacial adhesion of composites shows variation in thermal stability according to the MAPP type. Therefore, the thermal stability of MAPP is an important consideration for enhancement of the interfacial interaction of composites.

Table 2
Test results of M_w, MA graft (%), MFI, T_g and T_m of five different, commercially used, MAPP types

	M_w[a]	MA graft (%)[b]	MFI (g/10 min)	T_g (°C)	T_m (°C)
Polybond 3150	46,000	0.5	20	−24	165
Polybond 3200	42,000	1.0	104	−24	164
G-3003	52,000	1.2	90	−24	162
E-43	9100	1.2	ND	−25	154
Bondyram 1004	66,000	0.8	90	−23	160

[a] M_w of G-3003 and E-43 was obtained from Eastman Chemical Products Co.

[b] MA graft (%) of the five types of MAPP was obtained from Crompton Polybond Co. (Polybond 3150 and Polybond 3200), Eastman Chemical Products Co. (G-3003 and E-43) and Polyram Co. (Bondyram 1004), respectively.

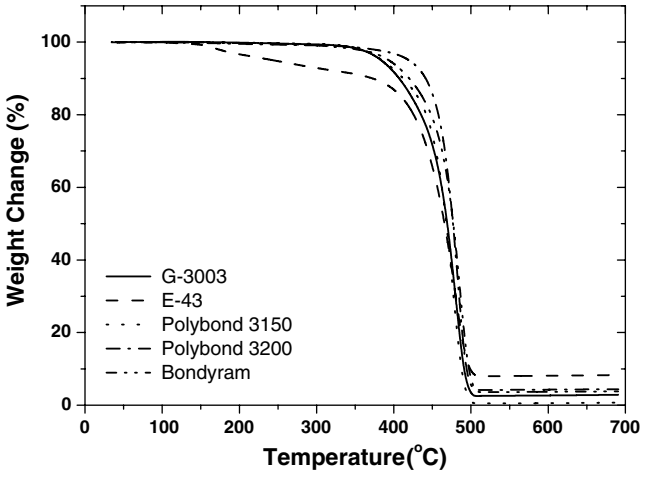

Fig. 1. TGA curves of G-3003, E-43, Polybond 3200 and Bondyram 1004 according to different MAPP types.

3.2. Mechanical properties

The tensile strength of RHF- and WF-filled PP composites is shown in Fig. 2 as a function of the filler loading. The tensile strength of the composites decreased with increasing bio-flour loading, due to the weak interfacial adhesion and low compatibility between the hydrophilic bio-flour and hydrophobic PP [2,8,12,19]. This result indicated that the impact and flexural strengths of the composites were slightly decreased with increasing bio-flour loading. The tensile strength of WF-filled PP composites was higher than that of RHF-filled PP composites, possibly due to the chemical constituents and particle size of bio-flour. The holocellulose and lignin content of WF is higher than that of RHF (Table 1). The bio-flour materials are mainly composed of a complex network of three polymers: cellulose, hemicellulose and lignin [12]. Lignin not only holds the bio-flour together, but also acts as a stiffening agent for the cellulose molecules within the bio-flour cell wall. Therefore, the lignin and cellulose content of bio-flour has an influence on the strength of bio-flour and the tensile strength of composites. The filler particle size of WF is smaller than that of RHF, and thereby offers a larger specific surface area and slightly increased interfacial interaction in the matrix polymer, compared to the larger RHF particle size, at the same weight fraction in the composites [3].

The tensile, impact and flexural strengths of the composites with different MAPP types are shown in Figs. 3–5, respectively. The tensile, impact and flexural strengths of the MAPP-treated composites were significantly greater than those of the MAPP non-treated composites due to the enhanced interfacial adhesion of the composites by MAPP. In addition, MAPP underwent esterification reaction or hydrogen bonding, at the interface, between the hydroxyl groups of the bio-flour on one side and the carboxylic groups of the MAPP diffused matrix polymer on the other side [8,9,18]. Figs. 3–5 show that the mechanical

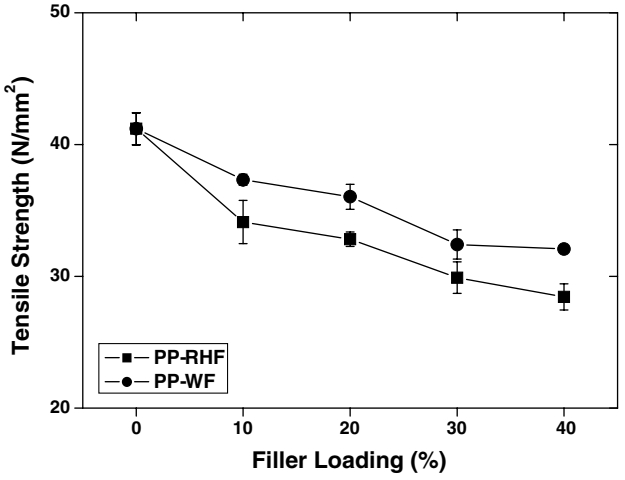

Fig. 2. Tensile strength of RHF- and WF-filled PP composites as a function of filler loading.

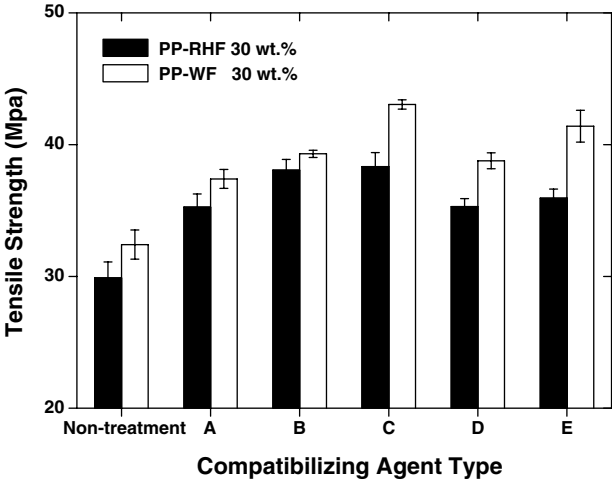

Fig. 3. Tensile strength of RHF- and WF-filled PP composites as a function of different MAPP types. A, Polybond 3150; B, Polybond 3200; C, G-3003; D, E-43; E, Bondyram 1004.

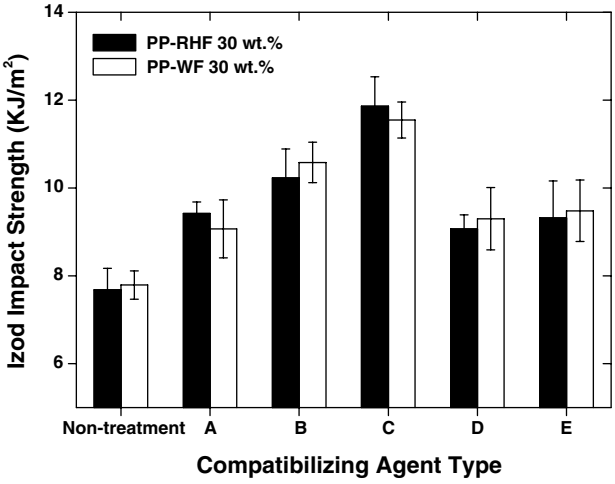

Fig. 4. Impact strength of RHF- and WF-filled PP composites as a function of different MAPP types. A, Polybond 3150; B, Polybond 3200; C, G-3003; D, E-43; E, Bondyram 1004.

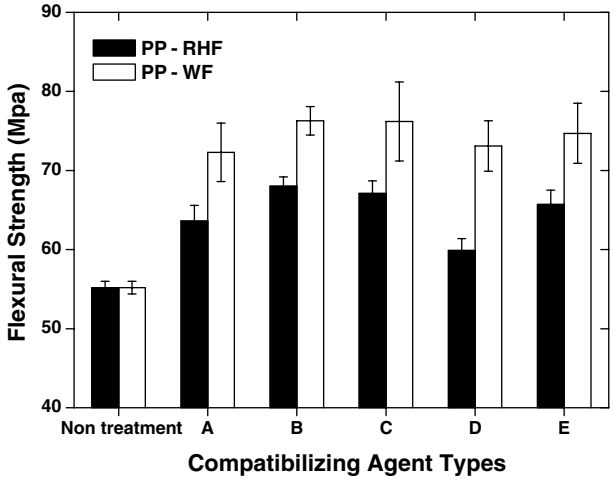

Fig. 5. Flexural strength of RHF- and WF-filled PP composites as a function of different MAPP types. A, Polybond 3150; B, Polybond 3200; C, G-3003; D, E-43; E, Bondyram 1004.

properties of the composites were affected by MAPP type. The tensile, impact and flexural strengths of G-3003-treated composites were the highest, probably because G-3003 contained sufficient M_w, as opposed to Bondyram 1004 which did not, and sufficient MA grafted on PP, compared to the insufficient level of Polybond 3150 and E-43. The sufficient M_w of MAPP allows better diffusion into the matrix polymer which indicates easier entanglement with the matrix polymer [6,15]. Furthermore, the sufficient number of MA groups attached onto the PP chains causes strong interfacial interaction, probably due to the formation of chemical bonds between MA groups and hydroxyl groups of bio-flours [3,17]. However, the tensile, impact and flexural strengths of Polybond 3150- and E-43-treated composites were the lowest, which was attributed to the low M_w (9100) of E-43 and too low MA graft (%) of Polybond 3150. Therefore, we concluded that the improvement in mechanical properties of the composites using MAPP as a compatibilizing agent was strongly dependent on the amount of MA graft (%) and the M_w of MAPP.

3.3. Morphological characterization

Figs. 6 and 7 show the SEM micrographs of the tensile fracture surfaces of MAPP non-treated and treated (G-3003) composites, respectively. In Fig. 6a, examination of the tensile fracture surface of MAPP non-treated composites indicated the presence of pulled-out traces and bigger gaps between the bio-flour and matrix, which is evidence of weak interfacial adhesion at the interface. Such weak interface between RHF and PP can be seen even more clearly in the SEM micrograph of greater magnification shown in Fig. 6b. Weak interfacial adhesion easily led to complete debonding from the matrix in the tensile fracture surface [18]. The SEM micrograph of G-3003-treated composites shown in Fig. 7a, along with the magnified

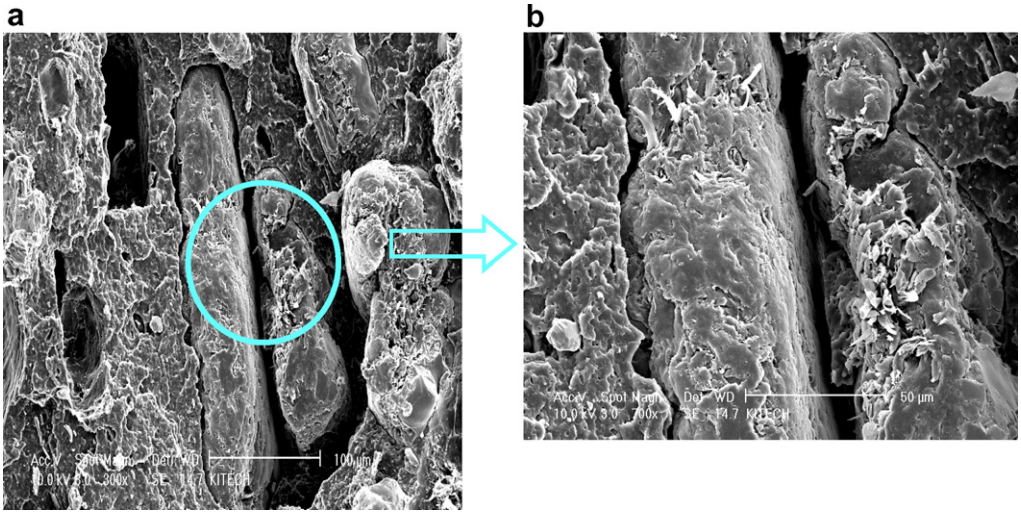

Fig. 6. SEM micrographs of the tensile fracture surface of MAPP non-treated, RHF-filled, PP composites: (a) 300× and (b) 700×.

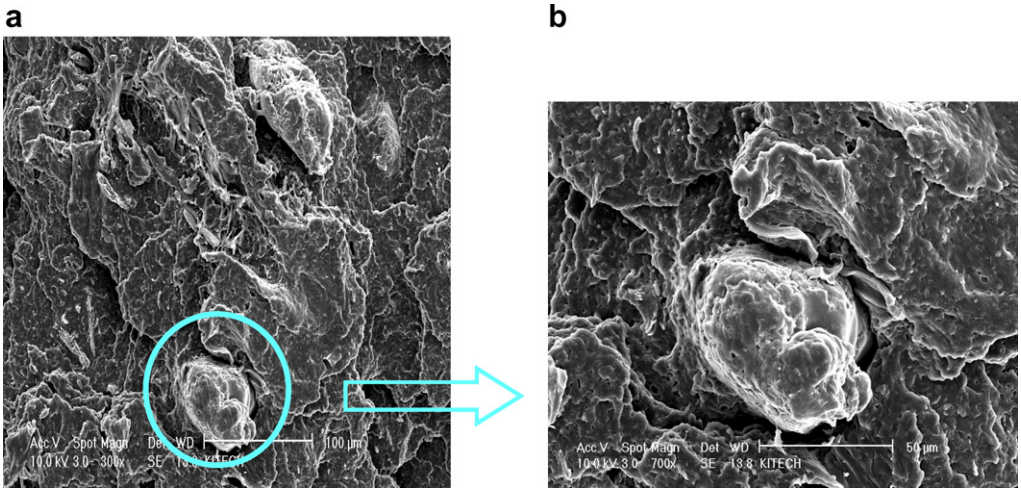

Fig. 7. SEM micrographs of the tensile fracture surface of MAPP (G-3003)-treated, RHF-filled, PP composites: (a) 300× and (b) 700×.

micrograph of Fig. 7b, clearly show the strong bonding and paucity of pulled-out traces from the matrix in the two phases. This result clearly demonstrated that the MAPP treatment of composites provides strong interfacial adhesion and good wetting, as evidenced by the almost complete absence of holes around the matrix and paucity of breaking of bio-flours during tensile fracture [20].

3.4. FTIR-ATR analysis

Fig. 8a and b show the FTIR-ATR spectra of G-3003, Bondyram 1004, MAPP (G-3003)-treated and non-treated composites. G-3003 and Bondyram 1004 showed two low absorption peaks at 1774 and 1778 cm^{-1}. These peaks were assigned to symmetric C=O stretching of MA functions grafted on PP [21]. This result indicated that the MA functional groups of MAPP can be reacted with the hydroxyl groups of the bio-flour to produce covalent bonding and esterification reaction [12,22]. This result was confirmed by the stretching vibration of the ester carbonyl groups (C=O) such as at 1741 cm^{-1} (PP–RHF) and 1739 cm^{-1} (PP–WF) which have resulted from esterification reaction between free OH groups of the bio-flour and the MA functional groups of MAPP [9,11,22]. Thus, the ester bonding of MAPP-treated composites offers better wettability and dispersion which can thereby improve the mechanical and thermal properties of the final product.

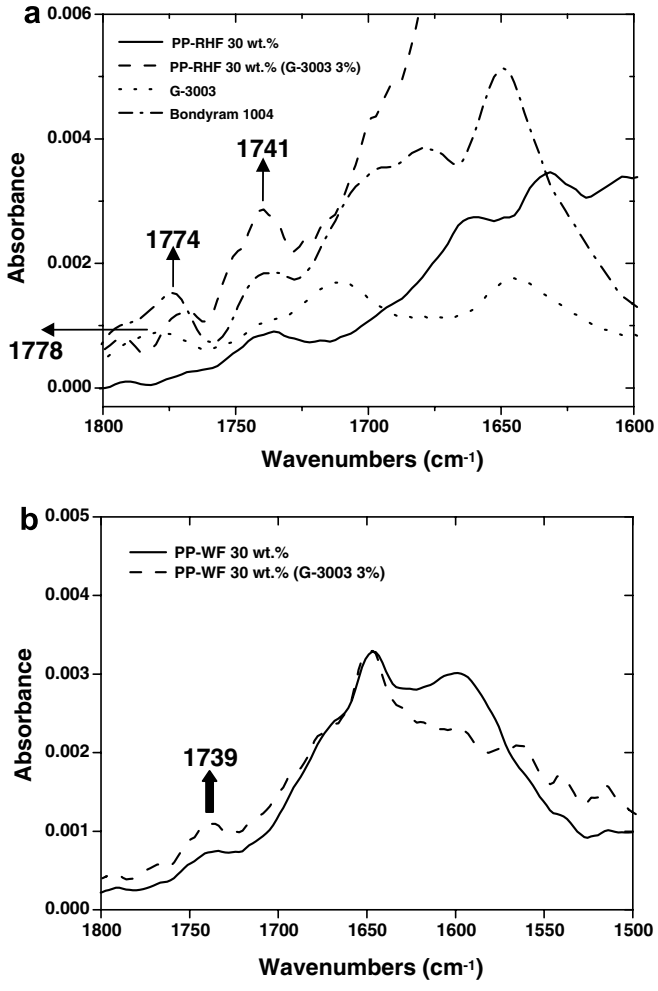

Fig. 8. FTIR-ATR spectra of MAPP (G-3003) non-treated and treated composites: (a) PP–RHF and (b) PP–WF.

3.5. Wide-angle X-ray scattering

The WAXS diffraction curves of PP, MAPP, MAPP (G-3003)-treated and non-treated composites taken by reflection mode are shown in Figs. 9 and 10, respectively. PP and MAPP showed strong diffraction peaks at 2θ of 14.1° (110), 16.8° (040), 18.4° (130) and 21.2° (111). These peaks were attributed to the (110), (040), (130) and (111) diffraction planes of the α-form of PP and MAPP crystals with a monoclinic configuration [23,24]. The hexagonal β-form of PP crystals with additional diffraction peaks at 2θ of 16° (300) was not evident, possibly

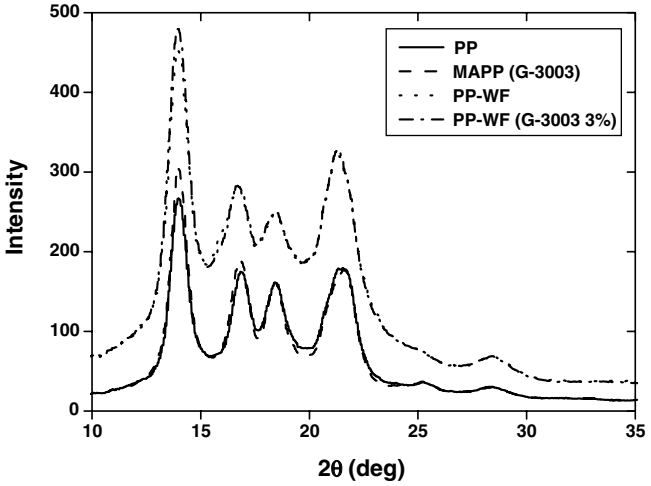

Fig. 9. WAXS diffraction curves of PP, MAPP (G-3003), MAPP non-treated and treated WF-filled PP composites.

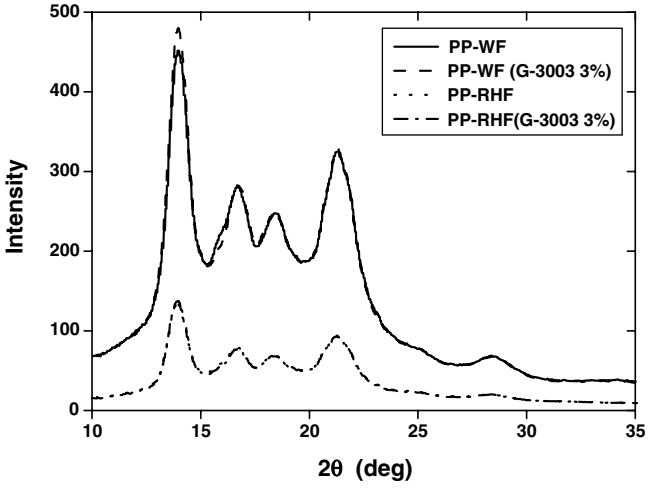

Fig. 10. WAXS diffraction curves of MAPP (G-3003) non-treated and treated composites.

due to the injection molding process of PP and MAPP at molten state for a certain time [24]. The same result was also seen in the composites and MAPP-treated composites. Pracella et al. [25] reported that no clear evidence of hexagonal β-modification was detected in Hemp fiber reinforced, PP composites and other PP composites reinforced with modified natural fibers. Table 3 shows the crystallinity of PP, G-3003, MAPP-treated and non-treated composites using XPS. The crystallinity of G-3003 and MAPP-treated composites was slightly higher than that of PP and MAPP non-treated composites, suggesting that the crystallization behavior of MAPP is slightly higher than that of PP due to chain branching of MA and the better dispersion of MAPP in the matrix polymer [25]. These results are presented in Table 4, which lists T_m, ΔH_f and X_c for PP, G-3003, MAPP-treated and non-treated composites obtained from the DSC second heating thermograms. T_m of PP, G-3003, MAPP-treated and non-treated composites was not significant changed but the X_c of G-3003 and MAPP-treated composites was slightly higher than that of PP and MAPP non-treated composites. The X_c of MAPP and MAPP-treated composites was higher in both DSC and XPS analyzer results. The crystallinity of PP–RHF and PP–WF composites was also seen in Tables 3 and 4. The crystallinity of PP–WF composites was much higher than that of PP–RHF composites. Wood and lignocellulosic materials are complex materials which consist mainly of cellulose, hemicellulose and lignin. Cellulose represents the crystalline structure of wood and lignocellulosic materials while the structures of hemicelluloses and lignin are amorphous [26]. In general, the content of proteins, organic acids, pectins, fat, and waxes of lignocellulosic materials is higher than that of wood. Therefore, the higher degree of crystallinity of lignocellulosic materials increases the removal of fat, wax, and amorphous materials by alkali treatment [27]. These results indicated that the crystallinity of RHF-PP composites is lower than that of WF-PP composites due to the higher content of amorphous materials and silica in RHF.

Table 3
Crystallinity (%) of PP, MAPP and composites

Sample	Crystallinity (%)
PP	43.5
MAPP (G-3003)	44.8
PP–RHF 30 wt%	32.6
PP–RHF 30 wt% (G-3003: 3%)	33.1
PP–WF 30 wt%	38.5
PP–WF 30 wt% (G-3003: 3%)	39.1

Table 4
Summary of T_m, ΔH_f and X_c for PP, G-3003 MAPP-treated and non-treated composites

Sample	T_m (°C)	ΔH_f (J/g)	Crystallinity (%)
PP	165.5	81.4	58.9
MAPP (G-3003)	162.2	83.9	60.8
PP–RHF 30 wt%	166.0	50.8	52.6
PP–RHF 30 wt% (G3003: 3%)	165.8	55.1	57.0
PP–WF 30 wt%	166.3	52.8	54.7
PP–WF 30 wt% (G3003: 3%)	165.2	59.1	61.2

3.6. Thermal stability: effect of processing temperature

The isothermal TGA method was used to measure the degradation temperature and weight loss caused by the actual processing temperature of the composites. The processing temperature of the composites is generally determined by the T_m of the matrix polymer. T_m of PP is between 160 and 170 °C. The processing temperature of the composites was set about 10–30 °C higher than the T_m of PP to obtain smooth manufacture of the composites. The weight loss of the composites was measured using the TGA isothermal method at a measuring temperature of under 180, 200 and 220 °C for 20 min. Figs. 11 and 12 show the isothermal TGA curves of the WF- and RHF-filled PP composites, respectively, under the consistent temperature of 180, 200 and 220 °C for 20 min. The ramping period to measure the isothermal condition and isothermal period for 20 min is shown in Fig. 11. In Figs. 11 and 12, the weight loss of composites was slightly increased with increasing isothermal test temperature and time. PP exhibited scarcely no weight change at these temperature [28]. The weight loss of composites at isothermal condition is due to the thermal degradation of the main constituents of bio-flour. Hemicellulose and lignin are two of the main constituents of bio-flour which have low thermal stability and degradation temperature compared to the matrix polymer [3,14,29]. The weight loss of composites at these isothermal and actual processing temperatures (180, 200 and 220 °C) are mainly affected by the hemicellulose and lignin of bio-flour [28,29]. Therefore, achieving the proper profile

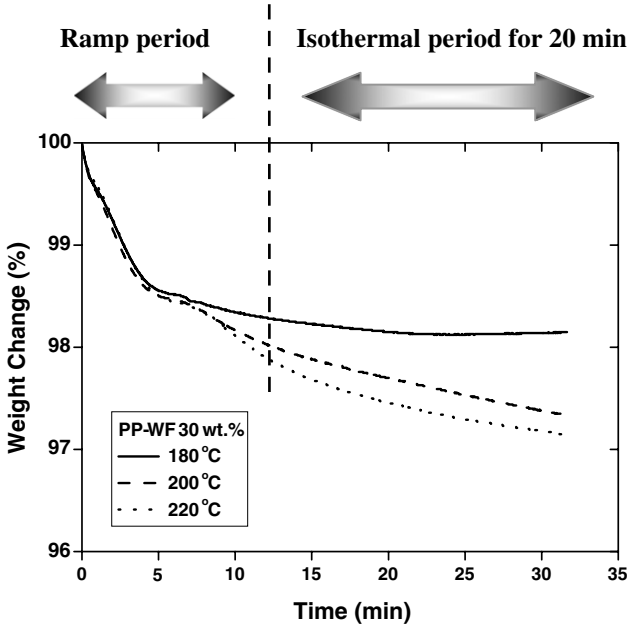

Fig. 11. Isothermal TGA curves of WF-filled PP composites.

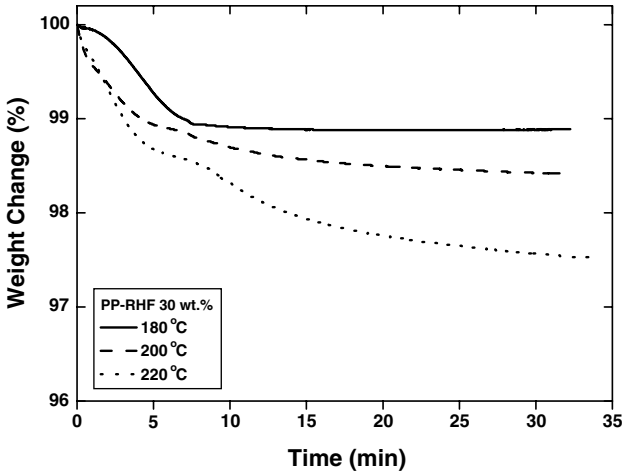

Fig. 12. Isothermal TGA curves of RHF-filled PP composites.

of temperature and time settings in the twin-screw extrusion process for the production of composites is important in order to prevent the degradation of mechanical properties of composites.

Fig. 13 presents the isothermal TGA curves of WF-filled PP composites with different MAPP types at 200 °C for 20 min. The weight loss of MAPP non-treated composites was slightly higher than that of MAPP-treated composites. The improved thermal stability of MAPP-treated composites was a result of the strong interfacial adhesion between the WF and PP that arose from the addition of the MA functional group of MAPP [14]. As shown in Fig. 13, the weight loss and thermal stability of the composites were slightly affected by the MAPP types. The weight loss of Bondyram 1004- and Polybond 3200-treated composites was slightly lower than that of G-3003- and E-43-treated composites, due to the higher thermal stability of the former two MAPP types that is evident in Fig. 1.

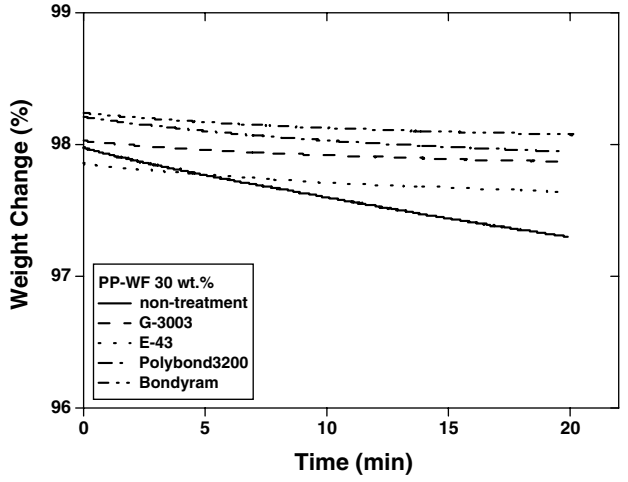

Fig. 13. Isothermal TGA curves of WF-filled PP composites as a function of different MAPP types at 200 °C.

4. Conclusions

The M_w of Bondyram 1004 and G-3003 and the MA graft (%) of G-3003 and E-43 were the highest, while the M_w of E-43 and MA graft (%) of Polybond 3150 were the lowest. Low M_w MAPP does not sufficiently entangle with the PP matrix and excessively high M_w MAPP may not allow the coupling agent to reside at the interface between MAPP and PP matrix. In addition, the low MA graft (%) of MAPP did not offer sufficient interaction between MAPP and bio-flour. Excessively high MA graft (%) of MAPP may hold the coupling agent too close to the hydrophilic surface and not allow sufficient interaction with the matrix. These results confirmed the non-optimum mechanical properties of MAPP-treated composites with excessively low or high M_w and MA graft (%). MAPP with lower M_w and polydispersity and higher MA graft (%) content showed higher MFI. The T_g and T_m did not show significant change according to MAPP type. The thermal stability of high M_w MAPP was superior to that of low M_w MAPP. The tensile, impact and flexural strengths of MAPP-treated composites were significantly increased compared to those of MAPP non-treated composites. This result was confirmed by the presence of pulled-out traces on the SEM micrographs of the tensile fracture surface between the bio-flour and matrix and by the FTIR-ATR spectral results for the stretching vibration of the ester carbonyl groups (C=O) such as at 1741 cm^{-1} (PP–RHF) and 1739 cm^{-1} (PP–WF).

The tensile, impact and flexural strengths of G-3003-treated composites were the highest and those of Polybond 3150- and E-43-treated composites were the lowest. The satisfactory G-3003 results were due to the sufficient level of M_w and MA grafted on PP for G-3003. The final properties and interfacial adhesion of MAPP-treated composites with sufficient M_w and MA graft (%) were superior to those of MAPP with low or excessively high M_w and MA graft (%). The crystallinity of MAPP and MAPP-treated bio-flour-filled PP composites was slightly higher than that of PP and MAPP non-treated composites. With increasing isothermal test temperature and time, the weight loss of composites was slightly increased. This result confirmed the importance of setting the proper temperature and time profiles for producing composites in the twin-screw extrusion in order to avoid the degradation of mechanical properties in the final products. The weight loss of MAPP non-treated composites was slightly higher than that of MAPP-treated composites. Furthermore, the weight loss of high M_w MAPP-treated composites was slightly lower than that of low M_w MAPP-treated composites.

Acknowledgement

This work was supported by the Brain Korea 21 project and by the Cleaner Production Technology Development project.

References

[1] Mohanty AK, Misra M, Drzal LT. Sustainable bio-composites from renewable resource: opportunities and challenges in the green materials world. J Polym Environ 2002;10:19–26.

[2] Yang HS, Kim HJ, Park HJ, Lee BJ, Hwang TS. Effect of compatibilizing agents on rice-husk flour reinforced polypropylene composites. Comp Struct 2007;77:45–55.

[3] Kim HS, Yang HS, Kim HJ. Biodegradability and mechanical properties of agro-flour–filled polybutylene succinate biocomposites. J Appl Polym Sci 2005;97:1513–21.

[4] Espert A, Camacho W, Karlson S. Thermal and thermomechanical properties of biocomposites made from modified recycled cellulose and recycled polypropylene. J Appl Polym Sci 2003;89: 2353–60.

[5] Kim HS, Yang HS, Kim HJ, Lee BJ, Hwang TS. Thermal properties of agro-flour-filled biodegradable polymer bio-composites. J Therm Anal Cal 2005;81:299–306.

[6] Panthapulakkal S, Sain M, Law S. Effect of coupling agents on rice-husk-filled HDPE extruded profiles. Polym Int 2005;54:37–142.

[7] Li Q, Matuana LM. Foam extrusion of high density polyethylene/ wood-flour composites using chemical foaming agents. J Appl Polym Sci 2003;88:3139–50.

[8] Tserki V, Matzinos P, Panayiotou C. Novel biodegradable composites based on treated lignocellulosic waste flour as filler. Part II. Development of biodegradable composites using treated and compatibilized waste flour. Compos Part A 2006;37:1231–8.

[9] Wu CS. Improving polylactide/starch biocomposites by grafting polylactide with acrylic acid-characterization and biodegradability assessment. Macromol Biosci 2005;5:352–61.

[10] Aziz SH, Ansell MP, Clarke SJ, Panteny SR. Modified polyester resins for natural fibre composites. Compos Sci Technol 2005;65: 525–35.

[11] Acha BA, Aranguren MI, Marcovich NE, Reboredo MM. Composites from PMMA modified thermosets and chemically treated woodflour. Polym Eng Sci 2003;43(5):999–1010.

[12] Marti-Ferrer F, Vilaplana F, Ribes-Greus A, Benedito-Borras A, Sanz-Box C. Flour rice husk as filler in block copolymer polypropylene: Effect of different coupling agents. J Appl Polym Sci 2005;99:1823–31.

[13] Yuan X, Jayaraman K, Bhattacharyya D. Effects of plasma treatment in enhancing the performance of woodfibre-polypropylene composites. Compos Part A 2004;35:1363–74.

[14] Joseph PV, Joseph K, Thomas S, Pillai CKS, Prasad VS, Groenincks G, Sarkissova M. The thermal and crystallization studies of short sisal fibre reinforced polypropylene composites. Compos part A 2003;34:253–66.

[15] Canche-Escamilla G, Cauich-Cupul JI, Mendizabal E, Puig JE, Vazquez-Torres H, Herrera-Franco PJ. Mechanical properties of acrylate-grafted henequen cellulose fibres and their application in composites. Compos Part A 1999;30:349–59.

[16] Keener TJ, Stuart RK, Brown TK. Maleated coupling agents for natural fibre composites. Compos Part A 2004;35:357–62.

[17] Baroulaki I, Karakasi Q, Pappa G, Tarantili PA, Economides D, Magoulas K. Preparation and study of plastic compounds containing polyolefins and post used newspaper fibers. Compos Part A 2006;37:1613–25.

[18] Demir H, Atikler U, Balkose D, Tihminlioglu F. The effect of fiber surface treatments on the tensile and water sorption properties of polypropylene-luffa fiber composites. Compos Part A 2006;37: 447–56.

[19] Plackett D. Maleated polylactide as an interfacial compatibilizer in biocomposites. J Polym Environ 2005;12:131–8.

[20] Malainine ME, Mahrouz M, Dufresne A. Lignocellulosic flour from cladodes of opuntia ficus-indica reinforced polypropylene composites. Marcromol Mater Eng 2004;289:855–63.

[21] Sclavons M, Laurent M, Devaux J, Carlier V. Maleic anhydride-grafted polypropylene: FTIR study of a model polymer grafted by ene-reaction. Polymer 2005;46:8062–7.

[22] Mohanty S, Verma SK, Nayak SK. Dynamic mechanical and thermal properties of MAPE treated jute/HDPE composites. Compos Sci Technol 2006;3–4:538–47.

[23] Nogales A, Hsiao BS, Somani RH, Srinivas S, Tsou AH, Balta-Calleja FJ, et al. Shear-induced crystallization of isotatic polypropylene with different molecular weight distribution: in situ small and wide-angle X-ray scattering studies. Polymer 2001;42:5247–56.

[24] Shangguan Y, Song Y, Peng M, Li B, Zheng Q. Formation of β-crystal from nonisothermal crystallization of compression-molded isotactic polypropylene melt. Eur Polym J 2005;41:1766–71.

[25] Pracella M, Chionna D, Anguillesi I, Kulinski Z, Piorkowska E. Functionalization, compatibilization and properties of polypropylene composites with hemp fibres. Compos Sci Technol 2006;13:2218–30.

[26] Wikberg H, Mauna SL. Characterisation of thermally modified hard- and softwoods by ^{13}C CPMAS NMR. Carbohyd Polym 2004;58: 461–6.

[27] Marcovich NE, Reboredo MM, Arangurn MI. Modified woodflour as thermoset fillers: II. Thermal degradation of woodflours and composites. Thermochim Acta 2001;372:45–57.

[28] Wielage B, Lampke Th, Marx G, Nestler K, Starke D. Thermogravimetric and differential scanning calorimetric analysis of natural fibres and polypropylene. Thermochim. Acta 1999;337:169–77.

[29] Siracusa G, La Rosa AD, Siracusa V, Trovato M. Eco-composites use of olive husk as filler in thermoplastic composites. J Polym Environ 2001;9:157–61.